LTD at amygdalocortical synapses as a novel mechanism for hedonic learning

Running title: Synaptic mechanisms for CTA learning

Melissa S. Haley, Stephen Bruno, Alfredo Fontanini and Arianna Maffei*

Affiliations. Dept. of Neurobiology and Behavior, SUNY – Stony Brook, Stony Brook, NY

Abstract: 207 words;
Text: 1789 words;
4 Figures;
Methods: 2534 words;
3 Extended Data Figures

Keywords: insular cortex, LTD, learning, plasticity, taste, conditioned taste aversion

Contributions. All authors were involved in writing and commenting the manuscript.
M.S. Haley designed and performed the experiments, analyzed the data and wrote the manuscript.
S. Bruno performed immediate early genes immunohistochemistry and cell counting.
A. Fontanini obtained funding, designed the study and wrote the manuscript.
A. Maffei obtained funding, designed the study, supervised experiments and analysis, and wrote the manuscript.

Send correspondence to: Arianna Maffei, Dept. of Neurobiology and Behavior, Life Science Building Rm 536, SUNY – Stony Brook, Stony Brook, NY 11794-5230. E-mail: Arianna.maffei@stonybrook.edu

Authors' disclosure: Alfredo Fontanini is a member of the scientific advisory board of Sage Therapeutics, Boston, MA

Acknowledgments: This work was supported by NIH-NIDCD awards DC013770, DC015234 to A. M. and A. F. We wish to thank Dr. Antonello Bonci for useful discussions and feedback on the study.

Abstract

Sensory stimuli are perceived and processed according to their physicochemical and affective signatures. For example, taste perception depends on the chemical identity of a tastant, as well as on its pleasantness or aversiveness. The affective value of a palatable gustatory stimulus changes if it becomes associated with gastric malaise, a phenomenon known as conditioned taste aversion (CTA)[1]. CTA depends on activity in the gustatory portion of the insular cortex (GC) and in the basolateral nucleus of the amygdala (BLA)[2,3]. Indeed, inactivation of GC or BLA impairs CTA[4-8]. Signaling mechanisms typically associated with induction of long term synaptic plasticity are engaged in this form of learning[9,10], suggesting that the shift in perception from pleasant to aversive depends on changes in synaptic efficacy. Here we report that CTA modulates synaptic drive onto GC pyramidal neurons, and that long term synaptic depression (LTD) at BLA - GC inputs is sufficient to change the hedonic value of a taste stimulus. Our results demonstrate a direct role for amygdalocortical LTD in taste aversion learning.

A novel, pleasant taste stimulus becomes aversive if associated with gastric malaise[1]. This effect is common to vertebrates and invertebrates and is an important survival response, as eating the wrong food may be deadly. In rodents, CTA can be induced by association of a sucrose solution (0.1M in water) with gastric malaise induced by an intraperitoneal (IP) injection of lithium chloride (LiCl, 0.15M, 7.5mL/kg body weight; **Fig. 1a**). In naïve rodents, a sucrose solution is preferable to water, however this preference shifts following the LiCl injection, as indicated by decreased consumption of sucrose compared to water in a 2-bottle test (**Fig. 1b**; Control, sucrose: 7.77 ± 0.34mL, water: 1.46 ± 0.24mL, N = 27; CTA, sucrose: 0.65 ± 0.11mL, water: 4.65 ± 0.22mL, N = 28; $p < 10^{-6}$). A significant difference in the aversion index (AI), calculated as ((water – sucrose)/total volume) (**Fig. 1c**; water preferred for $0 < AI < 1$; sucrose preferred if $-1 < AI < 0$), could be seen in animals in which the exposure to the tastant was followed by an IP injection of LiCl (**Fig. 1c**, CTA, AI: 0.75 ± 0.04, N = 28), compared to animals that received LiCl dissociated from the exposure to the tastant (**Fig. 1c**, control, AI: -0.69 ± 0.04, N = 27). To begin assessing the effects of CTA on GC activity, we quantified neurons expressing the immediate early genes c-Fos and EGR1 (**Fig. 1d-f**). We focused our analysis on pyramidal neurons in layers 2/3 of GC, as our previous work showed that they receive a powerful input from BLA[11]. There was a significant

decrease in the number of c-Fos and EGR1 positive neurons following CTA (**Fig. 1d-f**; c-Fos, control: 128.13 ± 9.46 positive nuclei/0.1mm^2, N = 6, CTA: 82.21 ± 11.73 positive nuclei/0.1mm^2, N = 6 rats, $p < 0.01$; EGR1, control: 175.90 ± 15.65 positive nuclei/0.1mm^2, N = 6, CTA: 133.03 ± 10.10 positive nuclei/0.1mm^2, N = 6, $p < 0.05$), suggesting that taste/malaise association decreased GC neurons activity, consistent with previous reports testing neuronal activity[2,12] and showing changes in markers for plasticity [10,13].

To determine whether CTA-induced decrease in IEG expression is related to the induction of plasticity in the GC circuit, we assessed whether CTA altered the excitability of GC neurons either by modulation of intrinsic excitability or as a consequence of synaptic changes. Rats were trained on the control or the CTA paradigm (**Fig. 1a**) starting at postnatal day 28 (P28). Following the 2-bottle test, acute slice preparations were obtained for patch clamp recordings [11]. To ensure that the 2-bottle test does not initiate CTA extinction, in a subset of rats we repeated the 2-bottle test on two consecutive days (**Extended data Fig. 1a**). The aversion indexes for sucrose on consecutive days were comparable (**Extended Data Fig. 1a**; AI day 1: 0.77 ± 0.08; AI day 2: 0.74 ± 0.08; N = 8; $p = 0.7$), excluding the possibility that an extinction process was initiated by the test.

All recorded neurons included in the analysis were in L2/3, showed pyramidal morphology, and were negative for GAD67 (**Fig 2a**). CTA did not affect GC neurons' input resistance and frequency/current injection (FI) curves (**Fig. 2b, c**; Control: n = 19; CTA: n = 19; $p = 0.5$). However, there was a significant reduction in spontaneous excitatory and inhibitory synaptic charge, with no net effect on the excitation/inhibition ratio (**Fig. 2d, e**; Control: n = 22; CTA: n = 22; $p = 0.3$). Additional analysis of spontaneous synaptic events unveiled a significant decrease in the cumulative amplitude distribution of spontaneous excitatory and inhibitory synaptic currents (sEPSCs and sIPSCs), but no change in their frequency (**Fig. 2f**; Control: n = 22; CTA: n = 22; $p = 0.7$). Average amplitude and frequency of sEPSCs and sIPSCs were not significantly affected, and the difference in the cumulative distribution was more marked for large events. Our results exclude the possibility that CTA altered intrinsic excitability and point to changes in synaptic efficacy as a mechanism for this learning paradigm. Furthermore, given that CTA-induced effects on synaptic drive were detectable in L2/3 pyramidal neurons sampled across the extent of GC, it is highly unlikely for them to depend on selective plasticity on a clustered subset of neurons [14].

Previous work demonstrated that CTA induction is impaired by inactivation of either GC or BLA[6-8], suggesting that the connection between these regions is a fundamental player in this form

of learning. The reduction in the distribution of large events we observed is consistent with the possibility that CTA may affect afferent inputs onto GC neurons, as these typically have larger amplitude than recurrent events[15,16]. We, therefore, asked whether the BLA-GC input onto pyramidal neurons may be affected by CTA using an optogenetic approach to activate BLA terminal fields in GC while recording pyramidal neurons in the superficial layers of GC. As extensively characterized in our previous study[11], we injected AAV9.CAG.ChR2-Venus.WPRE.SV40 [17] (University of Pennsylvania Vector Core; titer: 5.64^{12} particles/mL) in the BLA (2.1 mm posterior to bregma; 4.7 mm lateral to midline; 7.0 mm below the pia) of P14 rats. CTA training began 14 days after surgery. The position of the injection site (**Fig 3a**), and expression of the construct in BLA terminal fields within GC were verified histologically (**Extended Data Fig. 2a**). Consistency of expression across preparations was assessed as indicated in the Methods, shown in **Fig. 2a** of the **Extended Data**, and in our previous work[11,15,16,18]. Following the 2-bottle test, acute slices were prepared (1.5 mm to bregma) and patch clamp recordings were obtained from visually identified L2/3 pyramidal neurons. Brief (5 ms) pulses of blue light (470 nm) were delivered with an LED mounted on the fluorescence light path of an upright microscope and light-evoked excitatory postsynaptic currents (BLA-EPSCs) were recorded. The monosynaptic nature of BLA-EPSCs was verified as described in our previous work, and an input/output curve was obtained using light stimuli of increasing intensity (0.2 mW – 4.4 mW, measured at the output from the objective). As shown in **Fig 3b**, BLA-EPSCs amplitude was reduced following CTA (200.0 ± 32.8 pA, N = 11; n = 33; CTA: 104.0 ± 15.7 pA, N = 9; n = 31; $p < 0.01$), consistent with the reduction in spontaneous excitatory charge. As BLA provides a powerful glutamatergic input to L2/3 neurons[11], the decrease in BLA-EPSC amplitude may explain the reduced expression of IEGs in **Fig. 1d** and is consistent with reports of decreased GC neurons activity *in vivo*[2].

We hypothesized that the decrease in BLA-EPSC may be evidence for induction of long term depression (LTD) at BLA-GC synapses onto L2/3, and tested this possibility with an occlusion experiment[19-22]. If CTA and LTD at the BLA-GC input are related, further induction of LTD should be occluded in CTA trained rats. First, we needed to identify a pattern of activity that induced LTD at this synapse. The paradigm was designed based on phasic patterns of BLA neuron activity recorded *in vivo* in awake rodents[2,23]. The effect of such activity pattern on spontaneous GC activity was reported in our previous study[11]. The phasic induction pattern reliably induced

LTD at BLA-GC synapses (**Fig. 3e, f)** in 56.6% of the recordings from control rats. The remaining 43.4% of recordings showed either no change (21.7%) or potentiation (LTP, 21.7%), indicating that this pattern may be sensitive to changes in the excitability of GC neurons[24]. LTD induced by phasic BLA terminal field activation did not show changes in paired pulse ratio nor coefficient of variation (**Fig. 3e**), indicative of a postsynaptic site of plasticity expression[25,26], and consistent with the decrease in amplitude, but not frequency, of sEPSCs shown in **Fig. 2f**. LTD induction by phasic patterns of BLA terminal field activity in GC was occluded by CTA (**Fig. 3g, h**). After CTA, the proportion of recordings showing LTD in response to phasic BLA activity was reduced to 16.7% (from 56.6% in control; χ^2 $p < 0.02$), while that of recordings showing LTP increased to 50% (from 21.7% in control; χ^2 $p < 0.01$). The proportion of recordings in which induction produced no change in synaptic efficacy was not different from control (33.3%; χ^2 $p < 0.13$). We assessed the specificity of the occlusion by testing the effect of CTA on LTD induction with a different paradigm designed to mimic tonic BLA activity [2,23] (**Extended Data Fig. 3a, b)**. Tonic BLA activation induced LTD in 100% of the recordings in control rats (**Extended Data Fig. 3a**) and was not occluded by CTA (**Extended Data Fig. 3c**), indicating that CTA selectively affected the outcome of the phasic induction. These results strongly suggest that CTA and LTD induced by phasic BLA afferents activity are related.

Next, we asked whether phasic activation of BLA terminal fields in GC would be sufficient to induce CTA. To do that, we injected the AAV9.CAG.ChR2-Venus.WPRE.SV40 construct[17] (University of Pennsylvania Vector Core) construct in BLA and implanted an optic fiber (400 μm) in GC (**Fig. 4a**). As control, a group of animals was injected with an AAV9.hSyn.eGFP.WPRE.bGH construct (University of Pennsylvania Vector Core) and implanted with the optic fiber in GC. Both rat groups were trained on a modified CTA paradigm in which the LiCl-induced malaise was substituted with phasic activation of BLA terminal fields (**Fig. 4c**). As shown in **Fig. 4c**, light activation of BLA terminal fields in GC was sufficient to induce CTA in our experimental group. No aversion was induced in the control group as control maintained a very strong preference for sucrose in the 2-bottle test. Differently, rats which received phasic stimulation of the BLA-GC input showed no preference for sucrose over water. As shown in **Fig. 4d**, the AI measured following optogenetic induction of CTA is lower than that measured across all other CTA training conditions in which LiCl was used to induce the malaise (AI, control: -0.88 ± 0.01; opto-CTA: -0.21 ± 0.15; $p < 0.003$). Loss of preference, but lack of aversion was

expected, as LiCl induces a gastric malaise that is not present in animals that received light stimulation through the optic fiber during CTA training. GC receives extensive visceral innervation [27] which is not activated during BLA terminal fields stimulation. Nevertheless, phasic BLA terminal field stimulation alone changed the preference for the sucrose solution over water, indicating that plasticity at the BLA-GC input is sufficient for altering the hedonic value of a palatable taste stimulus.

Taste circuits are highly conserved among species, and changes in taste preference can be induced similarly in humans as well as many other organisms, making CTA and the amygdalocortical system ideal models for investigating neural mechanisms of hedonic learning. Our results link long term depression at the BLA-GC input to a change in taste preference, emphasizing how changes in synaptic efficacy underlie adaptive shifts in hedonic value capable of influencing perception and behavior.

References

1 Garcia, J., Kimeldorf, D. J. & Koelling, R. A. Conditioned aversion to saccharin resulting from exposure to gamma radiation. *Science* **122**, 157-158 (1955).

2 Grossman, S. E., Fontanini, A., Wieskopf, J. S. & Katz, D. B. Learning-related plasticity of temporal coding in simultaneously recorded amygdala-cortical ensembles. *J Neurosci* **28**, 2864-2873, doi:10.1523/JNEUROSCI.4063-07.2008 (2008).

3 Piette, C. E., Baez-Santiago, M. A., Reid, E. E., Katz, D. B. & Moran, A. Inactivation of basolateral amygdala specifically eliminates palatability-related information in cortical sensory responses. *J Neurosci* **32**, 9981-9991, doi:10.1523/JNEUROSCI.0669-12.2012 (2012).

4 Flynn, F. W., Grill, H. J., Schulkin, J. & Norgren, R. Central gustatory lesions: II. Effects on sodium appetite, taste aversion learning, and feeding behaviors. *Behav Neurosci* **105**, 944-954 (1991).

5 Cubero, I., Thiele, T. E. & Bernstein, I. L. Insular cortex lesions and taste aversion learning: effects of conditioning method and timing of lesion. *Brain Res* **839**, 323-330 (1999).

6 Bermudez-Rattoni, F. & McGaugh, J. L. Insular cortex and amygdala lesions differentially affect acquisition on inhibitory avoidance and conditioned taste aversion. *Brain Res* **549**, 165-170 (1991).

7 Braun, J. J., Slick, T. B. & Lorden, J. F. Involvement of gustatory neocortex in the learning of taste aversions. *Physiol Behav* **9**, 637-641 (1972).

8 Morris, R., Frey, S., Kasambira, T. & Petrides, M. Ibotenic acid lesions of the basolateral, but not the central, amygdala interfere with conditioned taste aversion: evidence from a combined behavioral and anatomical tract-tracing investigation. *Behav Neurosci* **113**, 291-302 (1999).

9 Martinez-Moreno, A., Rodriguez-Duran, L. F. & Escobar, M. L. Late Protein Synthesis-Dependent Phases in CTA Long-Term Memory: BDNF Requirement. *Front Behav Neurosci* **5**, 61, doi:10.3389/fnbeh.2011.00061 (2011).

10 Inberg, S., Elkobi, A., Edri, E. & Rosenblum, K. Taste familiarity is inversely correlated with Arc/Arg3.1 hemispheric lateralization. *J Neurosci* **33**, 11734-11743, doi:10.1523/JNEUROSCI.0801-13.2013 (2013).

11 Haley, M. S., Fontanini, A. & Maffei, A. Laminar- and Target-Specific Amygdalar Inputs in Rat Primary Gustatory Cortex. *J Neurosci* **36**, 2623-2637, doi:10.1523/JNEUROSCI.3224-15.2016 (2016).

12 Flores, V. L. *et al.* The role of the gustatory cortex in incidental experience-evoked enhancement of later taste learning. *Learn Mem* **25**, 587-600, doi:10.1101/lm.048181.118 (2018).
13 Gandolfi, D. *et al.* Activation of the CREB/c-Fos Pathway during Long-Term Synaptic Plasticity in the Cerebellum Granular Layer. *Front Cell Neurosci* **11**, 184, doi:10.3389/fncel.2017.00184 (2017).
14 Wang, L. *et al.* The coding of valence and identity in the mammalian taste system. *Nature* **558**, 127-131, doi:10.1038/s41586-018-0165-4 (2018).
15 Wang, L., Kloc, M., Gu, Y., Ge, S. & Maffei, A. Layer-specific experience-dependent rewiring of thalamocortical circuits. *J Neurosci* **33**, 4181-4191, doi:10.1523/JNEUROSCI.4423-12.2013 (2013).
16 Wang, L., Kloc, M., Maher, E., Erisir, A. & Maffei, A. Presynaptic GABAA Receptors Modulate Thalamocortical Inputs in Layer 4 of Rat V1. *Cereb Cortex*, doi:10.1093/cercor/bhx364 (2018).
17 Petreanu, L., Huber, D., Sobczyk, A. & Svoboda, K. Channelrhodopsin-2-assisted circuit mapping of long-range callosal projections. *Nat Neurosci* **10**, 663-668, doi:10.1038/nn1891 (2007).
18 Kloc, M. & Maffei, A. Target-specific properties of thalamocortical synapses onto layer 4 of mouse primary visual cortex. *J Neurosci* **34**, 15455-15465, doi:10.1523/JNEUROSCI.2595-14.2014 (2014).
19 Rioult-Pedotti, M. S., Friedman, D. & Donoghue, J. P. Learning-induced LTP in neocortex. *Science* **290**, 533-536, doi:10.1126/science.290.5491.533 (2000).
20 Crozier, R. A., Wang, Y., Liu, C. H. & Bear, M. F. Deprivation-induced synaptic depression by distinct mechanisms in different layers of mouse visual cortex. *Proc Natl Acad Sci U S A* **104**, 1383-1388, doi:10.1073/pnas.0609596104 (2007).
21 Maffei, A., Nataraj, K., Nelson, S. B. & Turrigiano, G. G. Potentiation of cortical inhibition by visual deprivation. *Nature* **443**, 81-84, doi:10.1038/nature05079 (2006).
22 Rodriguez-Duran, L. F., Castillo, D. V., Moguel-Gonzalez, M. & Escobar, M. L. Conditioned taste aversion modifies persistently the subsequent induction of neocortical long-term potentiation in vivo. *Neurobiol Learn Mem* **95**, 519-526, doi:10.1016/j.nlm.2011.03.003 (2011).
23 Parsana, A. J., Li, N. & Brown, T. H. Positive and negative ultrasonic social signals elicit opposing firing patterns in rat amygdala. *Behav Brain Res* **226**, 77-86, doi:10.1016/j.bbr.2011.08.040 (2012).
24 Abraham, W. C. & Bear, M. F. Metaplasticity: the plasticity of synaptic plasticity. *Trends Neurosci* **19**, 126-130 (1996).
25 Kessels, H. W. & Malinow, R. Synaptic AMPA receptor plasticity and behavior. *Neuron* **61**, 340-350, doi:10.1016/j.neuron.2009.01.015 (2009).
26 Malinow, R. & Malenka, R. C. AMPA receptor trafficking and synaptic plasticity. *Annu Rev Neurosci* **25**, 103-126, doi:10.1146/annurev.neuro.25.112701.142758 (2002).
27 Cechetto, D. F. & Saper, C. B. Evidence for a viscerotopic sensory representation in the cortex and thalamus in the rat. *J Comp Neurol* **262**, 27-45, doi:10.1002/cne.902620104 (1987).
28 Bekkers, J. M. & Delaney, A. J. Modulation of excitability by alpha-dendrotoxin-sensitive potassium channels in neocortical pyramidal neurons. *J Neurosci* **21**, 6553-6560 (2001).
29 Maffei, A., Nelson, S. B. & Turrigiano, G. G. Selective reconfiguration of layer 4 visual cortical circuitry by visual deprivation. *Nat Neurosci* **7**, 1353-1359, doi:10.1038/nn1351 (2004).
30 Jackman, S. L., Beneduce, B. M., Drew, I. R. & Regehr, W. G. Achieving high-frequency optical control of synaptic transmission. *J Neurosci* **34**, 7704-7714, doi:10.1523/JNEUROSCI.4694-13.2014 (2014).
31 Lin, J. Y., Lin, M. Z., Steinbach, P. & Tsien, R. Y. Characterization of engineered channelrhodopsin variants with improved properties and kinetics. *Biophys J* **96**, 1803-1814, doi:10.1016/j.bpj.2008.11.034 (2009).

Methods

Long Evans rats of both sexes were used for this study. Animals were singly housed in a vivarium on a 12h/12h light dark cycle with ad libitum access to food and water, except where otherwise noted. Experiments were conducted during the light period. All surgical and experimental procedures were approved by the Institutional Animal Care and Use Committee of Stony Brook University and followed the guidelines of the National Institutes of Health.

Conditioned taste aversion training. Rats were placed on water restriction with free access to food for a total of 8 days. Rats were habituated to a behavioral chamber where they had 15 min access to a drinking spout with H_2O, followed by 1 hour access to H_2O in their home cage four hours later. The volume consumed was recorded daily throughout training (total volume (ml): juveniles, 12.58 ± 0.38; adults, 16.88 ± 0.72), and rats' weight was monitored to ensure that it remained within 85% of initial weight. Four days of habituation training was sufficient to stabilize fluid intake levels (Habituation, **Fig. 1a**). This was followed by two conditioning trials, with a recovery day in between identical to the habituation days. The recovery day enabled us to confirm that the conditioning procedures did not affect thirst levels. For immunhistochemistry and slice electrophysiology, conditioning consisted of 15 min access to a drinking spout with 0.1 M sucrose, followed by an ip injection of 0.15 M LiCl (7.5 mL/kg) to induce gastric malaise. Rats in the control group received an ip LiCl injection (0.15 M) in the evening on day 4 and 6 of training. The injection was delivered approximately 16 hours before sucrose presentation to ensure lack of association between gastric malaise and sucrose consumption (**Fig 1a**, pseudo CTA). For experiments *in vivo*, conditioning consisted of 15 min access to a drinking spout with 0.1 M sucrose, followed by optogenetic stimulation of BLA terminal fields in GC. On the 8^{th} training day, all groups engaged in a 2-bottle test to assess a preference for H_2O or sucrose. In a subset of experiments, the 2-bottle test was repeated on day 9, to assess whether the first test had initiated an extinction process (**Extended Data Fig. 1a**).

Immunohistochemistry. Detection of immediate early genes expression - One hour after the 2-bottle test, rats were anesthetized and intracardially perfused with PBS followed by 4% paraformaldehyde in PBS (4% PFA). The brain was dissected out and thin (50µm) coronal slices containing GC were cut with a fixed tissue vibratome (Leica VT1000). Sections were washed in PBS (3 x 10 min rinse), permeabilized and blocked in a solution containing 0.5% Triton X and 10% normal goat serum in PBS for 1 h, then incubated overnight at 4°C in a solution containing

0.1% Triton X and 3% normal goat serum in PBS, mouse anti-GAD67 (1:500, MilliporeSigma, MAB5406, monoclonal), and either rabbit anti-cFos (1:500, Cell Signaling, 2250S, monoclonal) or rabbit anti-EGR1 (1:500, Cell Signaling, 4153S, monoclonal). Sections were then rinsed in PBS (3 x 10 min) and incubated at 25°C for 2 h in a solution containing 0.1% Triton X and 3% normal goat serum in PBS, goat anti-mouse Alexa Fluor-647 (1:500, Invitrogen, A21235), goat anti-rabbit Alexa Fluor-568 (1:500, Invitrogen, A11011), and NeuroTrace 435/455 (1:1000, Invitrogen, N21479). After a final wash in PBS (3 x 10 min), sections were mounted with Fluoromount-G (Southern Biotech). Sections were imaged with a confocal microscope (Olympus Fluoview) at 20x magnification. Four sections, spaced at 200 µm, were counted per animal for each IEG (cFos = 4, EGR1 = 4) using ImageJ software by a person blind to experimental condition. Cell counts represent the number of IEG-positive, GAD67-negative neurons, normalized by the counting area (L2/3 aGC) for each section.

Recovery of recorded neurons in acute slice preparation - Recorded slices were fixed in 4% PFA for 1 week. They were then washed in PBS (3 x 10 min rinse), permeabilized and blocked in a solution containing 1% Triton X and 10% normal goat serum in PBS for 2 h, then slices were incubated overnight at 4°C in a solution containing 0.1% Triton X and 3% normal goat serum in PBS, streptavidin Alexa Fluor-568 conjugate (1:2000, Invitrogen, S11226), mouse anti-GAD67 (1:500, MilliporeSigma, MAB5406, monoclonal), and chicken anti-GFP (1:1000, Abcam, ab13970, polyclonal). GC slices were then rinsed in PBS (3 x 10 min) and incubated at 25°C for 2 h in a solution containing 0.1% Triton X and 3% normal goat serum in PBS, goat anti-mouse Alexa Fluor-647 (1:500, Invitrogen, A21235), goat anti-chicken Alexa Fluor-488 (1:500, Abcam, ab150173), and Hoechst 33342 (1:5000, Invitrogen, H3570). BLA slices were incubated overnight at 4°C in a solution containing 0.1% Triton X and 3% normal goat serum in PBS and chicken anti-GFP (1:1000, Abcam, ab13970, polyclonal). They were then rinsed in PBS (3 x 10 min) and incubated at 25°C for 2 h in a solution containing 0.1% Triton X and 3% normal goat serum in PBS, goat anti-chicken Alexa Fluor-488 (1:500, Abcam, ab150173), and Hoechst 33342 (1:5000, Invitrogen, H3570). Validation of injection sites and positioning of fiber optics - Following behavioral training, animals were anesthetized and perfused intracardially with PBS followed by 4% PFA. Coronal slices containing BLA and GC were cut at 100 µm with a fixed tissue vibratome (Leica VT1000). All sections were washed in PBS (3 x 10 min rinse) and incubated at 25°C for 1 h in a solution containing 0.1% Triton X and Hoechst 33342 (1:5000, Invitrogen, H3570). Sections

were mounted with Fluoromount-G (Southern Biotech) and the accuracy of viral injections and fiber placements was assessed.

Electrophysiology. Acute coronal slices containing GC were obtained immediately following the 2-bottle test. Slice preparation was as described in our previous study[11]. Briefly, rats were anesthetized with isoflurane (Bell jar to effect) and rapidly decapitated. The brain was dissected in ice cold, oxygenated artificial cerebrospinal fluid (ACSF), and 300 µm coronal slices containing GC were prepared using a fresh tissue vibratome (Leica VT1000) starting at 1.5 mm to bregma. Patch clamp recordings were obtained from visually identified L2/3 pyramidal neurons under DIC optics. Their identity was tested online with the injection of square current pulses (700 ms) to assess regular firing patterns, and post-hoc with immunohistochemistry aimed at reconstructing neuron morphology, assessing location, and confirming lack of expression of the GABA neuron marker GAD67. To assess possible changes in intrinsic excitability induced by CTA, recordings were obtained in current clamp in the presence of fast synaptic receptor blockers (in µM: DNQX, 20; APV, 50; picrotoxin, 20) and square current pulses of increasing amplitude were injected to examine input resistance, action potential threshold, and frequency/intensity curves. Input resistance was calculated from the linear portion of the voltage response to a -50 pA current injection. Action potential threshold was calculated as the membrane voltage when the first derivative of the voltage trace dV/dt = 20 V/s[28]. In a different set of experiments, spontaneous synaptic activity was recorded in voltage clamp. For these experiments, a cesium sulfate-based internal solution containing the sodium channel blocker QX314 (2 mM, Tocris Bioscience) was used to stabilize recordings during prolonged depolarization. Spontaneous synaptic currents were recorded at three different holding potentials around the reversal potential for chloride (to record sEPSCs, in mV: -55, -50, -45) and around the reversal potential for AMPA and NMDA-mediated currents (to record sIPSCs, in mV: 0, +5, +10). Current versus voltage functions were used to identify the voltage that better isolated the current of interest, which were used for analysis of charge and spontaneous events' amplitude and frequency[11,29]. Total charge was calculated by integrating 5 s sections of the current trace. Evoked EPSCs/EPSPs from stimulation of BLA terminal fields were obtained in voltage clamp and current clamp using a potassium gluconate solution and holding neurons at -70mV. The monosynaptic nature of BLA-EPSCs was verified as in our previous study[11]. Event-triggered average of light-evoked BLA-EPSCs and BLA-EPSPs was used to align BLA-EPSC and BLA-EPSP onset and calculate the average amplitude of the

light-evoked response. Latencies of BLA-evoked responses were calculated from the onset of the phasic 5 ms light pulse. For plasticity experiments, 2 LED pulses (5 ms, 10 Hz) were used to elicit BLA-EPSCs every 30 s. A brief (10 ms) 1 mV depolarization step was used to monitor series resistance (R_s). After a 10 min baseline, either the phasic or tonic induction paradigm was applied in current clamp, after which BLA-EPSCs were recorded for an additional 40 min. Neurons with $R_s > 20$ MΩ or that changed >10% during recording were excluded from analysis.

Optogenetics. *Ex vivo* experiments: Rats (P14) were anesthetized intraperitoneally with a mixture containing 70 mg/kg ketamine, 0.7 mg/kg acepromazine, and 3.5 mg/kg xylazine (KXA), and mounted on a stereotaxic apparatus. Animals received an injection of the AAV9.CAG.ChR2-Venus.WPRE.SV40 construct[17] (University of Pennsylvania Vector Core) in the BLA using a nanoject pressure injector (Drummond Nanoject II;100 nL volume containing 5.64^{12} particles/mL) as described in our previous study[11]. The stereotaxic coordinates for the injections were 2.1 mm posterior to bregma; 4.7 mm lateral to midline; 7.0 mm below the pia. Rats were allowed to recover from surgery for 2 weeks before CTA training and recordings. AAV9 was chosen because it is primarily transported anterogradely, and because ChR2 expressed via AAV9 does not alter the short-term dynamics of evoked responses [30]. The lack of backfilled somata in all of our GC our preparations further confirms forward direction of transport and indicates that only BLA terminal fields in GC were activated by light pulses. Consistency of ChR2-Venus expression across preparation was as previously reported[11]. Briefly, as shown in **Fig. 2a** of the **Extended Data**, the intensity of the Venus signal in GC was quantified across a 500um wide region of interest (ROI) spanning the cortical mantle from the pia to L5/6 (included) across 10 preparations. The average and standard deviation of the fluorescent signal were plotted as a function of depth. The expression of the Venus signal was then assessed for all preparations used for electrophysiological recordings and compared to the calibration curve. Only data obtained from preparations with a fluorescence profile within 1 standard deviation of the average calibration curve were included in the analysis.

BLA-EPSCs were evoked with a 5ms light pulse delivered through the 40x objective mounted on an upright microscope (Olympus BX51WI). The intensity, frequency and timing of the blue light stimuli (470 nm) were controlled with an LED driver (ThorLabs). Intensity at the output was verified with a light meter (Thor Labs, Range: 0.2 - 4.4 mW). Phasic stimulation for plasticity induction was organized in 20 trains of 20-5 ms light pulses at 20 Hz delivered every 250 ms and paired with depolarization of the postsynaptic neuron with a 50 pA current step. Tonic activation

of BLA terminal fields was achieved using a ramping light stimulus (which prevented inactivation of ChR2 channels[31]. The duration of the ramping stimulus was 6 s from 0 to maximum (4.4 mW) light intensity and was controlled through the LED driver connected to an analog output of the amplifier. For plasticity induction, 10 ramping stimuli spaced 5 s were (**Extended Data Fig. 3**) paired with depolarization of the postsynaptic neuron with a 50 pA current step.

In vivo experiments: Stimulation of BLA terminal fields *in vivo* was achieved through optical fibers (Doric lenses, 400 μm) chronically implanted in GC (1.4 mm anterior to bregma; 5 mm lateral to midline; 4.5 mm below the pia). Rats, weighing > 250 g were anesthetized intraperitoneally with the KXA cocktail described above and supplemented with 40% of the induction dose as needed to maintain surgical levels of anesthesia. The scalp was exposed and holes were drilled for anchoring screws, optical fibers, and viral injection. The AAV9.CAG.ChR2-Venus.WPRE.SV40 construct[17] (University of Pennsylvania Vector Core) was bilaterally injected in the BLA (3.0 mm posterior to bregma; 5 mm lateral to midline; 7.2 mm below the pia) using a nanoject pressure injector (Drummond Nanoject II; 200 nL volume containing 5.64^{12} particles/mL) as described above. Optical fibers (Doric Lenses, 400 μm) were coated with DiI for better detection of the optic fiber tract and implanted bilaterally to target GC and were secured in place with dental cement.

For these experiments, recovery from surgery was 4 weeks prior to CTA training. The injection site in BLA and the positioning of the optic fiber in GC were verified histologically for each preparation. Stimulation was controlled via the digital output of a Multi-patch clamp amplifier (HEKA) and software (Patchmaster) and delivered through the implanted optical fibers coupled to a blue laser (Shanghai Dream, 470 nm). Light intensity at the tip of the optic fiber was measured with a light meter (6.5 mW, ThorLabs) The induction paradigm *in vivo* had the same structure as the phasic induction pattern used in slices (Trains of 20 pulses, in this case 10 ms long, at 20 Hz delivered every 250 ms, repeated 100 times) Animals received photostimulation immediately after exposure to the 0.1 M sucrose solution on conditioning days 1 and 2. A control group of rats received a BLA injection of the AAV9.hSyn.eGFP.WPRE.bGH construct (University of Pennsylvania Vector Core) to ensure that possible changes in sucrose preference were due to BLA terminal field stimulation and not to unspecific effects of the light stimulation.

Data analysis. Data were acquired with a HEKA 4 channels amplifier with integrated acquisition board. Data were sampled at 10 kHz. Patchmaster (WaveMetrix) was used as acquisition software.

Analysis was performed with custom procedures in Igor (WaveMetrix), Matlab, and Clampfit (Molecular Devices). Data were tested for normality, then the appropriate statistical test was chosen. Where appropriate, unpaired t-tests were applied, otherwise Mann-Whitney tests were applied. Multiple comparisons were assessed with OneWay ANOVA followed by post-hoc tests with Bonferroni correction. Cumulative distributions were compared using the 2-sample Kolmogorov-Smirnov (K-S) test. Linear regression analysis was used to determine correlations between BLA-EPSC/BLA-EPSP amplitude (**Extended Data Fig. 2d**, input/output function) and initial BLA-EPSC amplitude and induced plasticity (**Extended Data Fig. 3d**). For plasticity induction experiments, paired t-tests were used to detect significant differences between BLA-EPSC amplitude, PPR, and CV in the 10 min baseline period and in the 10 min period 30-40 min post-induction. Differences in probability of LTD vs LTP induction following CTA were assessed with χ^2 for contingency test. Significant differences were considered for $p < 0.05$.

Solutions. ACSF contained the following (mM): 126 NaCl, 3 KCl, 25 NaHCO3, 1 NaHPO4, 2 MgSO4, 2 CaCl2, 14 dextrose with an osmolarity of 315-325mOsm. The internal solution for analysis of excitability and evoked synaptic responses was as follows (mM): 116 K-Glu, 4 KCl, 10 K-HEPES, 4 Mg-ATP, 0.3 Na-GTP, 10 Na-phosphocreatine, 0.4% biocytin (V_{rev} $[Cl^{-1}] = -81$ mV). The pH of the internal solution was adjusted to 7.35 with KOH and the osmolarity adjusted to 295 mOsm with sucrose. The internal solution to assess spontaneous excitatory and inhibitory charge and events contained (mM): 20 KCl, 100 Cs-sulfate, 10 K-HEPES, 4 Mg-ATP, 0.3 Na-GTP, 10 Na-phosphocreatine, 3 QX-314 (Tocris Bioscience), 0.2% biocytin (Vrev [Cl−1] = −49.3 mV). *Drugs*. To assess the monosynaptic nature of BLA-EPSCs recordings were obtained in the presence of (in μM): 1 TTX (Tocris Bioscience), 100 4-aminopyridine (4-AP) (Tocris Bioscience). To determine possible changes in intrinsic excitability, the following blockers were bath applied (in uM): 20 DNQX (Tocris Bioscience), and 50 APV (Tocris Bioscience), 20 picrotoxin (Tocris Bioscience).

Figures and Figure Legends

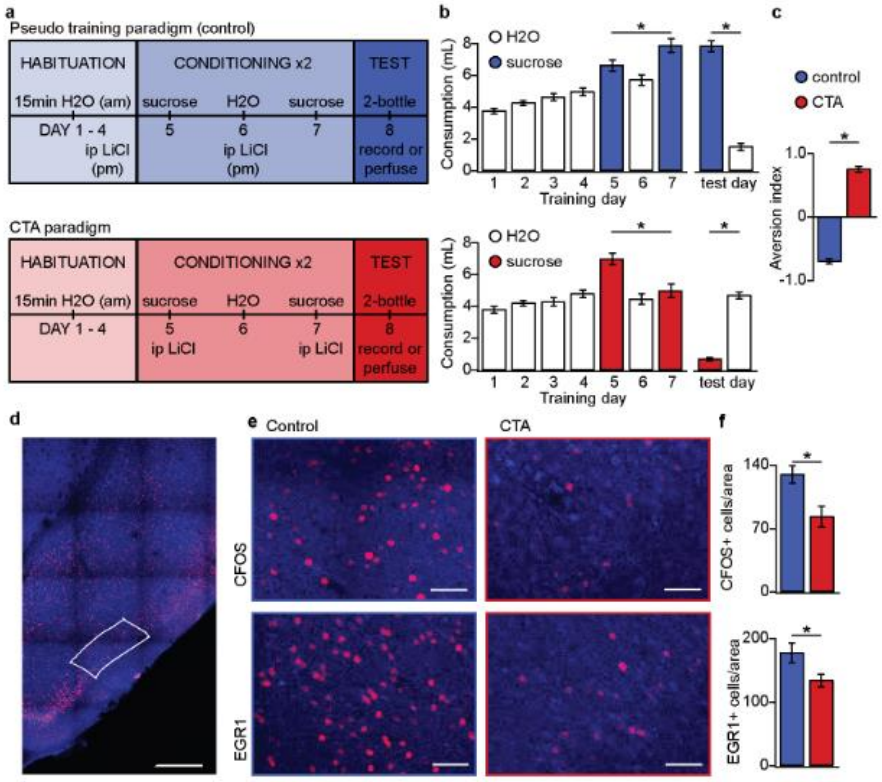

Figure 1: CTA learning decreases activation of excitatory neurons in L2/3 in aGC. a. Behavioral paradigm schematic. Top, blue: Control condition – animals (N = 27) received IP LiCl (10 mL/kg of 0.15 M LiCl) the evening prior to exposure to a sucrose solution (0.1 M). Bottom, red: CTA condition – animals (N = 28) received IP LiCl (7.5 mL/kg of 0.15 M LiCl) after sucrose exposure. **b.** Average fluid consumption across habituation days for each group was comparable (Control: 4.29 ± 0.18 mL/day; CTA: 4.21 ± 0.16 mL/day). Outline: H_2O, solid: sucrose; top: control group, bottom: CTA group. On the 2-bottle test, the control group drank on average 7.77 ± 0.34 mL of 0.1 M sucrose solution, while the CTA groups drank 0.65 ± 0.11 mL of the sucrose solution. **c.** Aversion index (Volume of water/Total volume consumed; Values > 0 indicate preference for water; Values < 0 indicate preference for sucrose) measured on test day for control group (blue; aversion index = -0.69 ± 0.04) and CTA group (red; aversion index = 0.75 ± 0.04). **d.** Representative image depicting region of interest (ROI, L2/3 aGC, white box). Scale bar = 500 μm. Red: immediate early gene; blue: Nissl counterstain. For details on imaging procedures see extended Methods. **e.** Representative images of c-Fos expression (top) and EGR1 expression (bottom) following 2-bottle testing from control group (left) and CTA group (right). Scale bar = 100 μm. **f.** Average counts of c-fos expressing (top; c-Fos, control: 128.13 ± 9.46 positive nuclei/0.1mm^2, N = 6, CTA: 82.21 ± 11.73 positive nuclei/0.1mm^2, N = 6 rats, $p < 0.01$) - and EGR1 expressing (bottom; EGR1, control: 175.90 ± 15.65 positive nuclei/0.1 mm^2, N = 6, CTA: 133.03 ± 10.10 positive nuclei/0.1mm^2, N = 6, $p < 0.05$) neurons normalized to the area of the ROI for control group (blue; N = 6 rats; n = 4 slices/rat;) and CTA group (red; N = 6 rats; n = 4 slices/rat). * indicates $p \leq 0.05$. Error bars ± SEM.

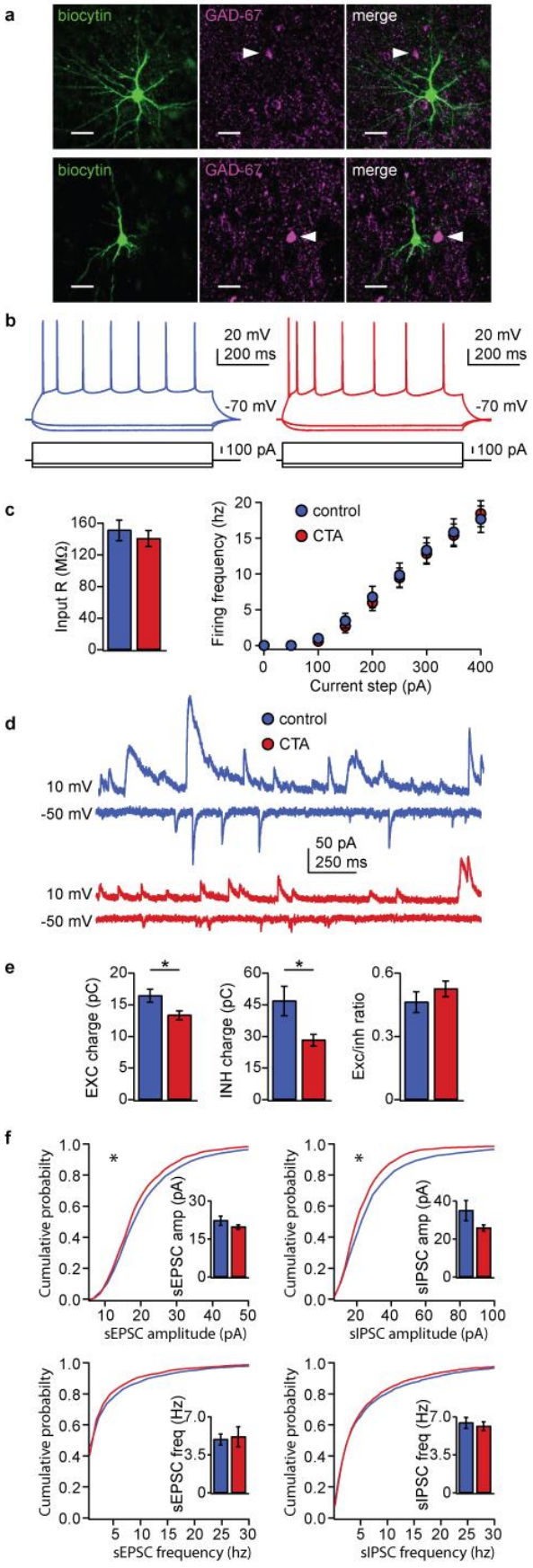

Figure 2: CTA induces changes in synaptic drive onto L2/3 pyramidal neurons in aGC. a. Images of example recorded neurons from a control animal (top) and CTA animal (bottom). Recorded neurons were identified as excitatory by their morphology (Left, biocytin: green) and lack of co-staining for GAD-67 (Middle, magenta). Right: merged images showing lack of co-localization of biocytin and GAD67. Scale bar = 25 µm. **b.** Steady-state firing patterns of neurons shown in a, showing no change in excitability. Left, control: blue; right, CTA: red. **c.** Average input resistance (left) and FI curves (right) for control group (blue) and CTA group (red). Neither parameter was affected by CTA (input resistance, Control: 149.43 ± 12.98 MΩ, N = 4 rats; n = 19 neurons; CTA: 139.26 ± 10.18 MΩ; p = 0.54, N = 4 rats, n = 19 neurons; FI slope, Control: 0.06 ± 0.01; CTA: 0.06 ± 0.01, p = 0.91). **d.** Sample traces of sIPSCs (top, holding = 10 mV) and sEPSCs (bottom, holding = -50 mV) onto a control neuron (blue) and CTA neuron (red). **e** Summary of EXC charge, INH charge, and E/I balance for control group (blue; EXC: 16.3 ± 1.0 pA/ms; INH: 46.3 ± 7.0 pA/ms; E/I ratio: 0.38 ± 0.05, N = 6 rats, n = 22 neurons) and CTA group (red; EXC: 13.2 ± 0.07 pA/ms; INH: 27.8 ± 2.8 pA/ms; E/I ratio: 0.39 ± 0.04; Control vs CTA, EXC: $p < 0.02$; INH: $p < 0.02$; E/I ratio: 0.93). **f.** Cumulative probability plots for sEPSC amplitude (top, left; 100 events/neuron, K-S test, Control vs CTA: $p < 10^{-6}$), sIPSC amplitude (top, right; 100 events/neuron; K-S test, Control vs CTA: $p < 10^{-6}$), sEPSC frequency (bottom, left; K-S test, Control vs CTA: $p = 0.3$), and sIPSC frequency (bottom, right; 100 events/neuron; K-S test, Control vs CTA: $p = 0.5$). Insets represent average values for control group (blue; sEPSC, amplitude: 22.03 ± 1.8 pA, frequency: 4.88 ± 0.50 Hz; sIPSC, amplitude: 34.74 ± 5.37 pA, frequency: 6.38 ± 0.50 Hz) and CTA group (red; sEPSC amplitude: 19.53 ± 0.86 pA, frequency: 5.13 ± 0.91; sIPSC, amplitude: 25.69 ± 1.58 pA, frequency: 6.08 ± 0.41Hz; Control vs CTA, sEPSC amplitude: $p = 0.22$; sEPSC frequency: $p = 0.81$; sIPSC amplitude: $p = 0.12$; sIPSC frequency: $p = 0.65$). * indicates $p \leq 0.05$. Error bars ± SEM.

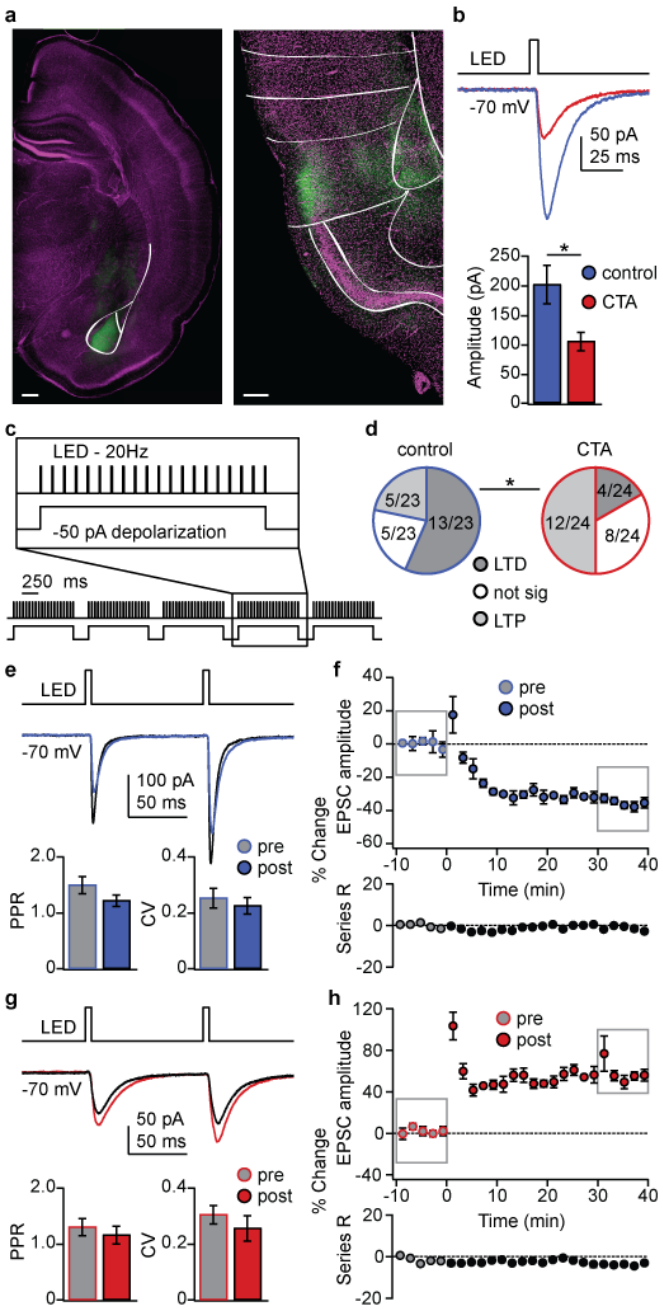

Figure 3: CTA decreases BLA-EPSC amplitude and occludes LTD onto L2/3 pyramidal neurons in aGC. a. Example of histological verification of injection site and expression of opsin construct in BLA terminal fields in aGC. Left: Image of ChR2-Venus expression at BLA injection site (scale bar = 500 µm); right: image of ChR2-Venus expression of BLA afferent fibers in aGC (scale bar = 250 µm; green: ChR2-Venus, magenta: Hoechst). **b.** Top: Sample traces of optogenetically-evoked BLA-EPSCs. Bottom: Summary of BLA-EPSC amplitude onto control neurons (blue; 200.0 ± 32.8 pA, N = 11 rats; n = 33 neurons) and CTA neurons (red; 104.0 ± 15.7 pA, N = 9 rats; n = 31 neurons; Control vs CTA: $p < 0.01$). **c.** Schematic of 20 Hz plasticity induction paradigm. BLA terminal fields were activated with 20 bursts of 20 light pulses (5 ms) at

20 Hz delivered every 250 ms (Top), while the postsynaptic neuron was depolarized subthreshold by injection of a 50 pA current step (Bottom). **d.** Distribution of the outcome of plasticity induction across all neurons recorded. Left: Control; right: CTA. Dark gray: LTD (Control: 56.6% of neurons; CTA: 16.7% of neurons; Chi Square test, $p < 0.02$), light gray: LTP (Control: 21.7%; CTA: 50%; $p < 0.01$), white: no change (Control: 21.7%; CTA: 33.3%; $p = 0.13$). **e.** Sample traces of BLA-EPSCs (top) and population PPR (bottom, left,) and CV (bottom, right) before (gray) and after (blue) 20 Hz plasticity induction in control group. PPR, baseline: 1.48 ± 0.15, post-induction: 1.20 ± 0.10; $p = 0.1$; CV, baseline: 0.25 ± 0.04, post-induction: 0.22 ± 0.03; $p = 0.49$; N = 11 rats; n = 23 neurons. **f.** Time course of change in BLA-EPSC amplitude (top) and series resistance (bottom) following 20 Hz LTD induction in control group. Boxes indicate pre- and post-induction epochs. The induction paradigm induced a 36.63 ± 5.12% decrease in BLA-EPSC amplitude. **g.** Sample traces of BLA-EPSCs (top) and summary of PPR (bottom, left) and CV (bottom, right) before (gray) and after (red) 20 Hz plasticity induction in CTA group. PPR, baseline: 1.29 ± 0.16; post-induction: 1.15 ± 0.16; $p = 0.1$; CV, baseline: 0.30 ± 0.03; post-induction: 0.25 ± 0.05; $p = 0.4$; N = 9 rats, n = 24 neurons. **h.** Time course of change in BLA-EPSC amplitude (top) and series resistance (bottom) following 20 Hz LTP induction in CTA group. Boxes indicate pre- and post-induction epochs. The induction paradigm induced a 58.76 ± 10.71% increase in BLA-EPSC amplitude. * indicates $p \leq 0.05$. Error bars ± SEM.

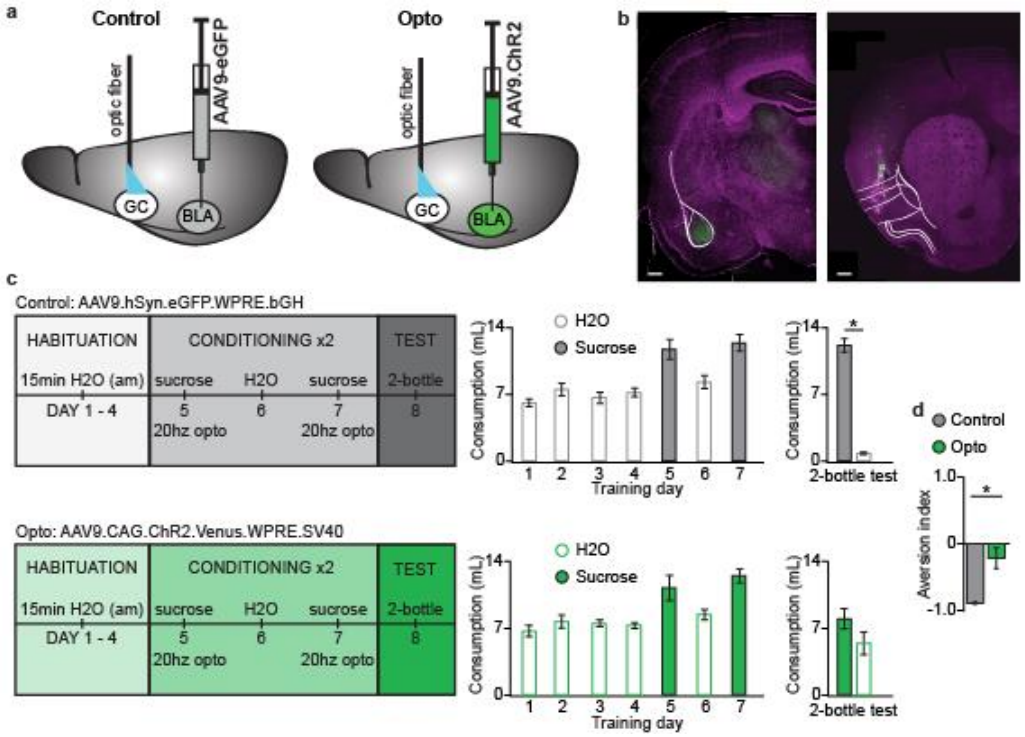

Figure 4: BLA terminal field activation *in vivo* with the phasic 20 Hz pattern eliminated sucrose preference. a. Cartoon of experimental approach. AAV9.hSyn.eGFP.WPRE.bGH: (Control group) or AAV9.CAG.ChR2-Venus.WPRE.SV40 (Opto group) were injected in BLA and an optic fiber (400 µm diameter, coated with DiL) was implanted in aGC. **b.** Correct positioning of injection site in BLA and of optic fiber in aGC were verified histologically. Left, green: injection site of ChR2-Venus; magenta: Hoechst counterstain; Right, green DiL indicating optic fiber tract; magenta: counterstain. White lines delineate anatomical landmarks indicating the location of BLA (left) and GC (right) based on the rat brain atlas (Paxinos and Watson, 1998). Scale bar = 500 µm. **c.** Left: diagram of behavioral paradigm for CTA in which the LiCl injection was substituted with 20 Hz optogenetic stimulation of BLA terminal fields in GC following sucrose exposure. To control for non-specific effects of light stimulation, the training was performed in 2 groups of rats, one injected with an AAV9 construct containing only the fluorescent tag Venus (Control, N = 8 rats) and one injected with the ChR2-Venus construct (Opto, N = 8 rats). Average fluid consumption across training days for each group (outline: H_2O, solid: sucrose; gray: Control group, green: Opto group). Both rat groups showed comparable water consumption on training days (Control: 6.87 ± 0.41 mL; Opto: 7.23 ± 0.21 mL; $p = 0.45$), and similar sucrose consumption on conditioning days (Control, conditioning day 1: 11.60 ± 1.01 mL, conditioning day 2: 12.27 ± 0.86 mL; Opto, conditioning day 1: 11.10 ± 1.30 mL, conditioning day 2: 12.36 ± 0.73 mL; Opto vs Control, conditioning day 1: $p = 0.8$, conditioning day 2: $p = 0.9$) excluding potential confounds due to neophobia. The two groups showed significant differences in the 2-bottle test (right). Control rats consumed more sucrose and less water, while Opto rats consumed less sucrose and more water compared to control (sucrose, Control: 12.03 ± 0.73 mL, Opto: 7.91 ± 1.07, $p < 0.008$; water, Control: 0.77 ± 0.12 mL, Opto: 5.35 ± 1.18 mL, $p < 0.006$). **d.** Right:

average aversion index on test day for Control (gray; -0.88 ± 0.01) and Opto (green; -0.21 ± 0.15; opto vs control: $p < 0.003$) rats. * indicates $p \leq 0.05$. Error bars ± SEM.